

Osteology of *Quasipaa robertingeri* (Anura: Dicroglossidae)

Meihua ZHANG¹, Xiaoping CHEN² and Xiaohong CHEN^{1*}

¹ Department of Zoology, College of Life Sciences, Henan Normal University, Xinxiang 453007, Henan, China

² School of Science and Technology, Jiaozuo Teachers College, Jiaozuo 454000, Henan, China

Abstract The objectives of this study are to present a detailed and comprehensive description of the osteology of *Quasipaa robertingeri* (Anura: Dicroglossidae), to provide osteological evidence for taxonomy, and to explore the adaptive traits of *Q. robertingeri*. We comprehensively studied the osteology of 2 adult specimens (1 male 98A00351 and 1 female 98A0041) of *Q. robertingeri* using conventional methods. Our osteological examination of *Q. robertingeri* shows that 1) the nasals are large and connect with one another medially; 2) the sphenethmoid is completely covered by the nasals and the frontoparietals, and thus it is not exposed dorsally; 3) the vomerine teeth are well-developed; 4) the anterior parts of the diapophyses of the presacral II protrude forward in the male, the same observation was made in the presacral II and III in the female; 5) the pectoral girdle is firmisternal; 6) the omosternum is fan-shaped posteriorly, and almost equal to the length of the mesosternum; 7) the xiphisternum is W-shaped with a deep incision posteriorly; 8) the humerus of the male is more developed in the crista ventralis, the crista medialis, and the crista lateralis; 9) the metacarpal II of the male presents with a nuptial tuber; and 10) the distal phalanges of the digits are anchor-shaped. Ultimately, the unique characteristics listed are most likely adaptations to the environment and amplexus of *Q. robertingeri*.

Keywords *Quasipaa robertingeri*, osteological characteristics, sexual dimorphism, environment, adaptation

1. Introduction

Morphology is primarily comprised of the external morphology, interior morphology, genital structure, embryology, and karyology (Xiong, 2008). Of these morphological components, the osteological characteristics of the interior morphology are comparatively conservative, and are thus utilized frequently for the taxonomic diagnoses of species, genera, and families, as well as for constructing phylogenetic relationships (Fei *et al.*, 2009; Hoyos, 2015; Lehr and Trueb, 2007; Trueb, 1973; Wei *et al.*, 2009). Additionally, habitat environment and behaviors can be extrapolated through osteological features, which is of great significance when the goal is to ascertain adaptive evolution.

In vertebrate evolution, anurans were one of the earliest landing groups and were capable of inhabiting various

environments, such as fossorial, terrestrial, aquatic, and arboreal environments (Duellman and Trueb, 1986; Fei *et al.*, 2009; Inger, 1967). Within the bounds of their unique shape, morphological differences in the hyoid, larynx, sacrum, girdle, limb proportions, and terminal phalanges likely enabled anurans to navigate different surroundings (Duellman and Trueb, 1986; Jorgensen and Reilly, 2013; Kent and Miller, 1997; Lynch, 1969; Simons, 2008; Tihen, 1965; Trueb, 1973).

Quasipaa robertingeri (Anura: Dicroglossidae) is endemic to China and inhabits mountainous streams and surrounding riparian areas at elevations of 650–1500 meters (Fei *et al.*, 2012). To date, this species has been recorded in Hejiang County and Changning County, in Sichuan Province (Fei *et al.*, 2009), Wenxin County, in Yunnan Province (Li *et al.*, 2009), and Chongqing City (Huang *et al.*, 2010). *Q. robertingeri* is classified as endangered because of its declining numbers (Wang and Xie, 2009). *Quasipaa* was recognized as a distinct subgenus and was subsequently elevated to the genus status mainly based on its external morphology, lacking adequate osteological data (Dubois, 1992, 2005).

* Corresponding authors: Prof. Xiaohong CHEN, from Henan Normal University, Xinxiang, Henan, China, with her research focusing on the evolution of anurans.

E-mail: xhchen-xx@sohu.com

Received: 13 November 2015 Accepted: 19 January 2016

The objectives of this study are to present a detailed and comprehensive description of the osteology of *Q. robertingeri*, to provide osteological evidence for taxonomy, and to explore the adaptive traits of this species.

2. Materials and Methods

We examined 2 adult specimens (1 male 98A00351 and 1 female 98A0041) of *Q. robertingeri* in this study. Both of the specimens were collected from the type locality in Hejiang County, Sichuan Province, China, during the 1998 breeding season. The specimens were euthanized in the laboratory and fixed in 10% neutral buffered formalin.

We dissected the frogs by hand using a dissecting microscope. We documented the dissection process with photographs taken using a digital microscope combined with a Nikon D7100 camera. We used Photoshop CS5 to combine the photos into a single figure. We adopted general osteological terminology from Trueb (1973), Duellman and Trueb (1986), and Fabrezi (1992). The terminology we use for the hyoid and larynx follows Trewavas (1933). All of the osteological features we discuss herein are based on the female *Q. robertingeri* specimen, unless we specify otherwise.

3. Results

The osteology is generally comprised of the axial skeleton and the appendicular skeleton. The axial skeleton includes the skull, the vertebral column, and the sternum. The appendicular skeleton includes the girdles, and the limbs.

3.1 Axial Skeleton

3.1.1 Skull The skull of *Q. robertingeri* is arc-shaped anteriorly, and wider than its length (Figure 1A, B).

Nasals: The nasals are large, funnel-shaped, and cover two-thirds of the nasal capsules dorsally. They articulate with one another medially and reach the frontoparietals posteriorly. The maxillary process of the nasal is long, tapered, and extend laterally to the preorbital process of the pars facialis of the maxilla. They contribute to the anterior margin of the orbit (Figure 2A).

Nasal cartilages: The bodies of the nasal cartilages are situated between the premaxillae and the sphenethmoid, and have 3 paired differentiated rami. Dorsally, the front parts of the nasal cartilages extend anterolaterally and form the anterior wall of the nasal cavity. Ventrally, the front margins of the cartilages extend 2 short club-shaped rami and attach to the alary processes of the premaxillae. The rear parts of the cartilages extend laterally to the pars

palatina of the maxillae, support the maxillary processes of the nasals, and contribute to the anterior walls of the orbits. The rear parts of the cartilages then embed into the grooves of the anterior rami of the pterygoids.

Septomaxillae: The septomaxillae are small and lodged in the bottom of the external nares between the nasals and the maxillae; they are not in contact with any bones. The inner border of the bone is arc-shaped with a medial projection. The posterior edge is triangular (Figure 2B, C).

Sphenethmoid: The tubular sphenethmoid forms the anterolateral walls of the braincase. From the dorsal view, the bone is completely hidden by the nasals and the frontoparietals. The sphenethmoid is ventrally supported by the cultriform process of the parasphenoid. The posterior end of the bone bears an inverted U-shaped incision dorsally, and an inverted V-shaped incision ventrally (Figure 2D).

Frontoparietals: The frontoparietals roof the braincase and are slightly wider posteriorly than anteriorly. They articulate with the nasals anteriorly, and posteriorly with the exoccipitals and the prootics (Figure 2E).

Prootics: The prootics are large, form the posterolateral walls of the braincase, and house the auditory capsules. The elements dorsomedially articulate with the frontoparietals and the exoccipitals. Laterally, they are invested by the squamosals and the pterygoids (Figure 2F, G, H).

Exoccipitals: The exoccipitals form the posteriormost parts of the braincase, and the posteromedial walls of the auditory capsules. Medially, the exoccipitals encircle the foramen magnum. Posteriorly, the elements bear a pair of occipital condyles and jugular foramen (Figure 2I, J).

Vomers: The vomers obliquely lie anterior to the palatines. The anterior process of the vomer is moderately expanded and points anterolaterally. The prechoanal process is long, thin, orients laterally, and supports the anterior end of the choana. The postchoanal process is broad, robust, slants posterolaterally, and supports the posterior end of the choana. The medial process of the vomer is a roughly rectangular lamina. The dentigerous process bears approximately 7 vomerine teeth (Figure 2K).

Parasphenoid: The sword-like parasphenoid supports the braincase ventrally. The anterior tip of the cultriform process is pointed, extends to the level of the anterior margin of the orbit, and connects with the vomers and palatines. The alae orient laterally, perpendicular to the cultriform process. The posteromedial process of the parasphenoid is short and invests the ventral surface of

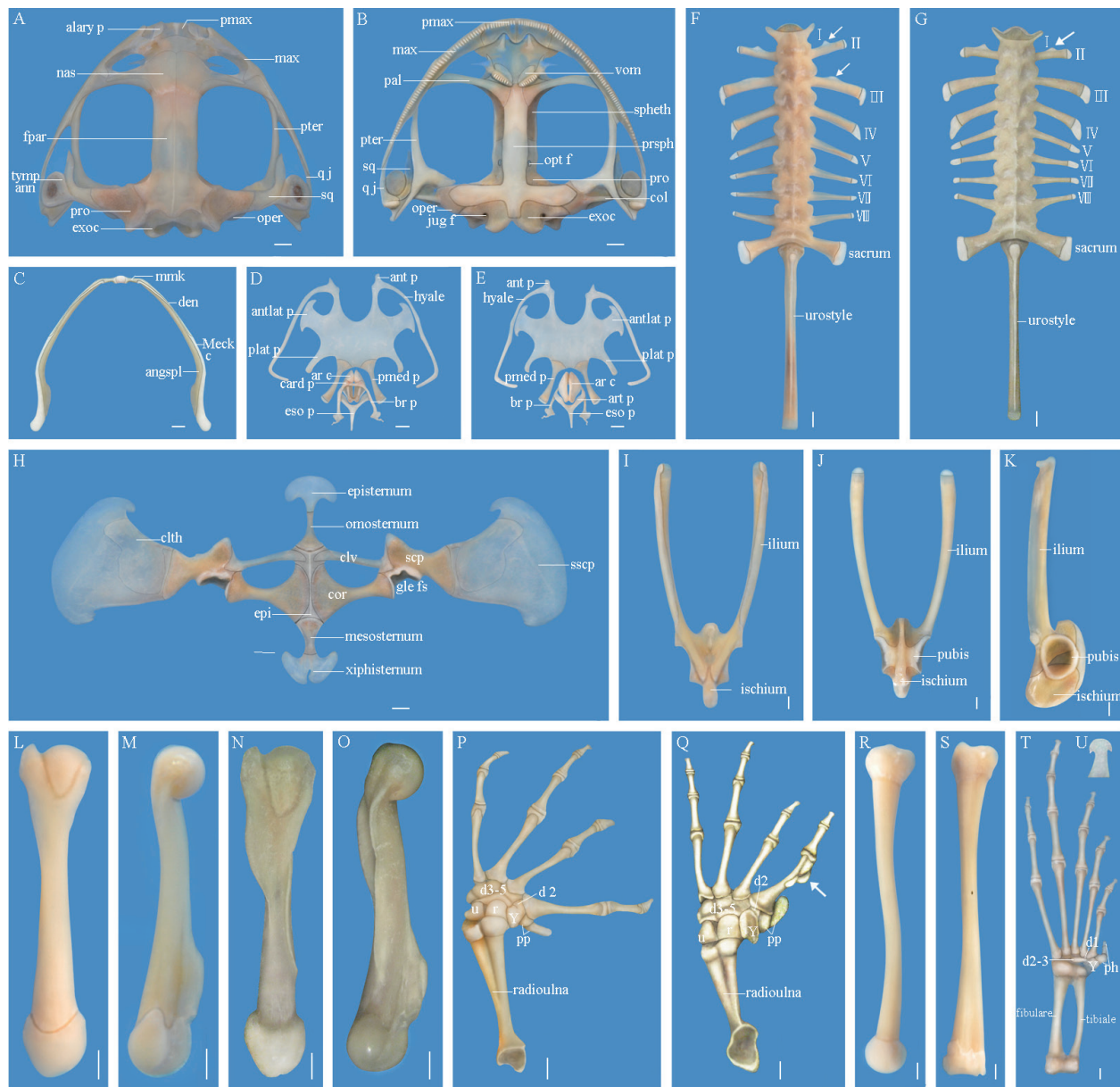


Figure 1 Osteology of *Quasipaa robertingeri*, specimen 98A0041, adult female. A: skull, dorsal view; B: skull, ventral view (abbreviations: alary p, alary process; col, columella; exoc, exoccipital; fpar, frontoparietal; jug f, jugular foramen; max, maxilla; nas, nasal; pal, palatine; oper, operculum; opt f, optic foramen; pmax, premaxilla; pro, prootic; prsph, parasphenoid; pter, pterygoid; qj, quadratojugal; spheth, sphenethmoid; sq, squamosal; tym ann, tympanic annulus; vom, vomer); C: mandible, dorsal view (abbreviations: ang spl, angulosplential; den, dentary; Meck c, Meckel's cartilages; mmk, mentomeckelian); D: hyoid apparatus and laryngeal apparatus, dorsal view; E: hyoid apparatus and laryngeal apparatus, ventral view (abbreviations: ant p, anterior process; antlat p, anterolateral process; plat p, posterolateral process; pmed proc, posteromedial process; ar c, arytenoid cartilage; art p, articular process; br p, bronchial process; card p, cardiac process; eso p, esophageal process); F: vertebral column, dorsal view; G: vertebral column of the male, dorsal view; H: pectoral girdle, ventral view (abbreviations: clth, cleithrum; clv, clavicle; cor, coracoid; epi, epicoracoid; gle fs, glenoid fossa; scp, scapula; sscp, suprascapula); I: pelvis girdle, dorsal view; J: pelvis girdle, ventral view; K: pelvis girdle, lateral view; L: humerus, rear view; M: humerus, dorsal view; N: humerus of the male, rear view; O: humerus of the male, dorsal view; P: forearm and hand, dorsal view (abbreviations: d2, distal carpal 2; d3-5, distal carpal 3+4+5; pp, prepollex; r, radiale; u, ulnare; Y, Y element); Q: forearm and hand of the male, dorsal view (white arrow shows the nuptial tuber); R: femur, dorsal view; S: tibiofibula, ventral view; T: foot, dorsal view (abbreviations: d1, distal tarsal 1; d2-3, distal tarsal 2+3; ph, prehallux); U: distal phalanx of toe III, dorsal view. Scale bar = 2 mm.

the exoccipitals (Figure 2L).

Palatines: The palatines are distinctly arcuate and long. They articulate with the cultriform process of the parasphenoid medially and laterally with the pars palatina

of the maxillae. They contribute to the anterior parts of the orbits (Figure 2M).

Columellae: The rod-shaped columella is situated ventral to the crista parotica. It consists of 2 components:

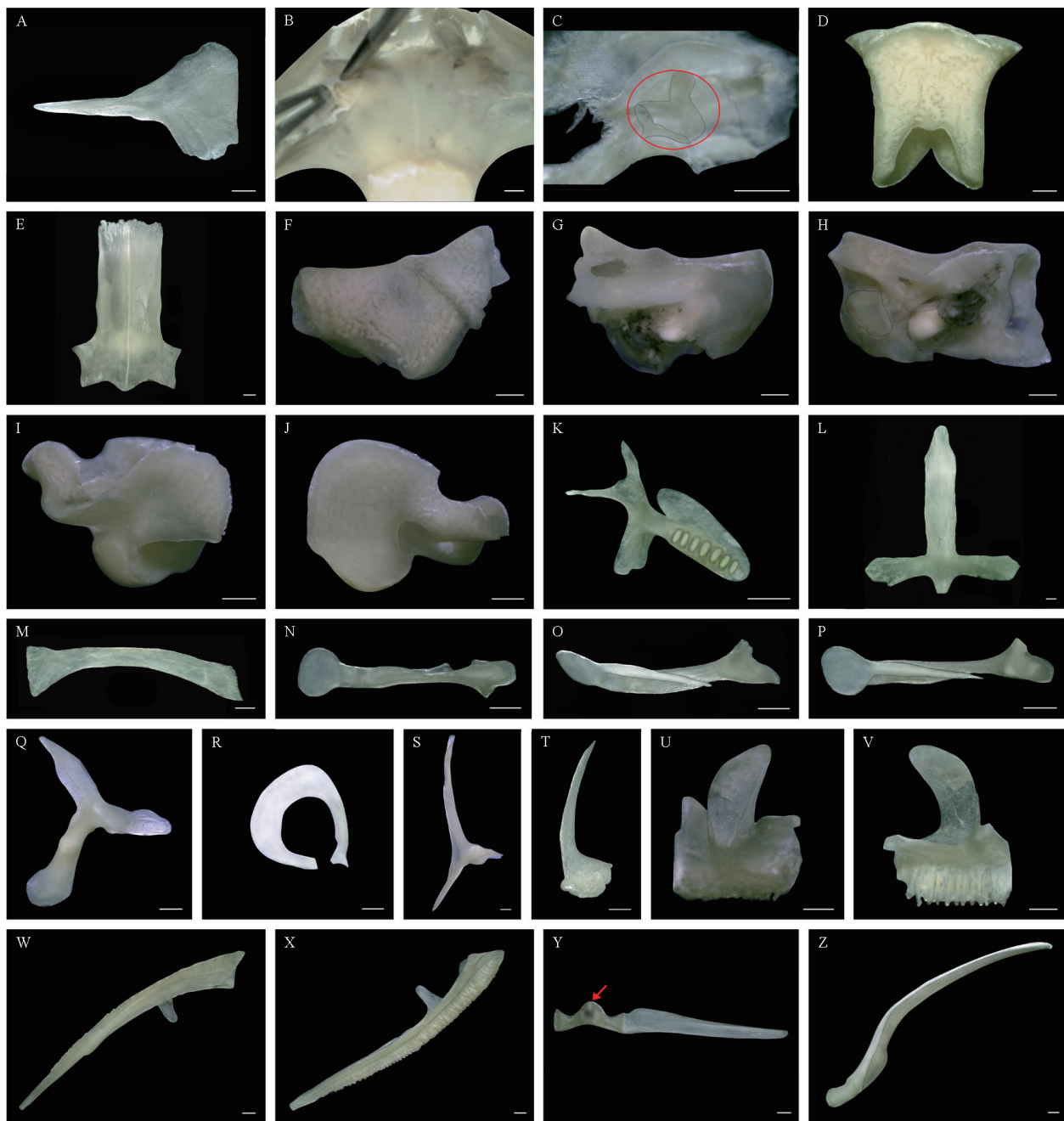


Figure 2 Skull elements of *Quasipaa robertingeri*, specimen 98A0041, adult female. A: left nasal, dorsal view; B: nasal region, dorsal view; C: left septomaxilla (Its inner and outer borders were separated from one another by external force), dorsal view; D: sphenethmoid, dorsal view; E: frontoparietals, dorsal view; F: left prootic, dorsal view; G: left prootic, ventral view; H: left prootic, rear view; I: left exoccipital, dorsal view; J: left exoccipital, ventral view; K: left vomer, dorsal view; L: parasphenoid, dorsal view; M: left palatine, dorsal view; N: left columella, rear view; O: left columella, lateral view; P: left columella, front view; Q: left squamosal, dorsal view; R: left tympanic annulus, dorsal view; S: left pterygoid, dorsal view; T: left quadratojugal, dorsal view; U: left premaxilla, front view; V: left premaxilla, rear view; W: left maxilla, dorsal view; X: left maxilla, ventral view; Y: a pair of mentomeckelians and a single dentary (the red arrow shows the spherical cartilage), front view; Z: angulosplenial and Meckel's cartilage, dorsal view. Scale bar = 1 mm.

(1) the ossified portion and (2) the cartilaginous portion. The ossified portion has a triangle expansion at its proximal end and is adjacent to the operculum. Its distal end supports the plate-shaped cartilage, which distally passes through the tympanic annulus and attaches to the

tympanic membrane. The plate-shaped cartilage medially separate into a tapering ramus that extends along the slant groove of the ossified portion (Figure 2N, O, P).

Squamosals: Each squamosal consists of 3 rami: (1) the zygomatic ramus, (2) the otic ramus, and (3) the

ventral ramus. The zygomatic ramus is blade-shaped and projects anterodorsally. The otic ramus articulates with the lateral margin of the prootic. The ventral ramus covers the posterior part of the quadratojugal (Figure 2Q). The tympanic annulus lies between the zygomatic ramus and the ventral ramus of the squamosal (Figure 2R).

Pterygoids: The triradiate pterygoids are well-developed, and underlie the squamosals in the dorsal aspect. The anterior ramus is the longest ramus, extends along the pars palatina of the maxilla and forms the lateral wall of the orbit. The medial ramus articulates with the anterolateral tip of the prootic but does not connect with the ala of the parasphenoid. The posterior ramus extends to the jaw joint. Notably, both the anterior rami and posterior rami of the pterygoids bear longitudinal grooves laterally (Figure 2S).

Maxillary Arch

Premaxillae: The premaxillae are the anteriormost elements of the maxillary arches, connect with one another medially, and connect laterally with the maxillae. Each premaxilla is composed of the tooth-bearing pars dentalis, the pars palatina, and the alary process. The alary process, which is a posterior concave lamina, extends dorsally and its terminal margin inclines laterally. The pars dentalis is dentate. The pars palatina, which points posteriorly, is perpendicular to the pars dentalis and is medially concave (Figure 2U, V).

Maxillae: The maxillae are the largest components of the maxillary arches, articulate with the premaxillae anteriorly, and posteriorly overlap the anterolateral surface of the quadratojugals. The pars dentalis bears numerous aligned teeth. Both the pars palatina and pars facialis are wide and well-developed. The preorbital process of the pars facialis is present and roughly rectangular (Figure 2W, X).

Quadratojugals: The quadratojugals complete the maxillary arches posteriorly. The anterior part of the bone is thin and unites with the maxilla. The posterior portion is broad, thick, and covered by the ventral ramus of the squamosal (Figure 2T).

Quadrates: The quadrates are supported by the ventral rami of the squamosals dorsally, and the posterior rami of the pterygoids medially, and the quadratojugals laterally. Functionally, the quadrates join with the mandible.

Mandible (Figure 1C and Figure 2Y, Z)

Mentomeckelians: The mentomeckelian forms the anterior side of the mandible. The bone attaches to the spherical cartilage medially, and laterally articulates with the dentary and the Meckel's cartilage.

Angulosplenials: The angulosplenial forms the internal

border of the mandible and encloses the medial surface of the Meckel's cartilage.

Dentaries: The dentary forms nearly half of the external edge of the mandible. Anteriorly, the bone is synostotically united to the mentomecklian. Posteriorly, it is free and covers the Meckel's cartilage anterolaterally.

Meckel's cartilages: The Meckel's cartilage (throughout almost the entire mandible) anteriorly articulates with the mentomeckelian. Posteriorly, it joins with the quadrate of the maxillary arch.

Hyoid Apparatus (Figure 1D, E)

Hyoid plate: The width of the hyoid plate is roughly 1.6 times its medial length. The hyoid plate is measured from the medial point between the posteromedial processes to the anteromedial edge of the hyolaryngeal sinus, and across the narrowest point underneath the alary processes (Scott, 2005). The hyolaryngeal sinus is narrow and U-shaped. It is deeper than the anterior side of the base of the anterolateral (alary) process. The anterolateral processes (with a broad stalk) are large, and wider distally than proximally. The posterolateral processes are slender, and posteriorly direct inward.

Hyales: The hyales are long, bowed, and distally extend to the otic capsules. The anterior processes are short and curve laterally.

Posteromedial processes: The posteromedial processes are bony, long, noticeably broader anteriorly than posteriorly, and end in cartilage. They embrace the laryngeal apparatus.

Laryngeal Apparatus (Figure 1D, E)

Arytenoids: The arytenoids are crescent-shaped and have narrow corners dorsally and ventrally. Together, the arytenoids form a hollow hemispherical chamber. The apexes of the arytenoids are unclosed and form the glottis. The vocal cords lie dorsomedial to the margin of the arytenoids.

Cricoid: The cricoid forms a complete ring, and supports the arytenoids. The muscular processes and the lateral processes are absent. The articular processes are low, while the cardiac processes are well-developed. The posterior ends of the bronchial processes are expanded triangular-shaped, which attaches to the anterior parts of the lungs. The esophageal process is long, tapered, and associated with the ventral wall of the esophagus.

3.1.2 Vertebral Column The vertebral column is composed of 8 presacral vertebrae, the sacrum, and the urostyle, all of which are imbricate (Figure 1F).

Cervical vertebra: The cervical vertebra, namely the presacral I, bears a pair of cervical cotyles anterolaterally, which articulate with the occipital condyles of the

exoccipitals. Ventrally, the anterior tip of the cervical vertebra is convex and projects into the foramen magnum.

Trunk vertebrae: The presacral II–VII are procoelous, while the presacral VIII is amphicoelous. The transverse processes of the presacrals II–IV are more robust than those of the presacrals V–VIII. The relative lengths of the transverse processes of the trunk vertebrae are $\text{III} > \text{IV} > \text{V} > \text{VI} > \text{VII} > \text{VIII} > \text{II}$. The diapophyses of the presacrals II and VIII direct anteriorly. The diapophyses of the presacral VII are perpendicular to the body axis. The other diapophyses of the presacrals all slant posteriorly.

Curiously, the medial anterior margins of the diapophyses of the presacral II protrude forward in the male (Figure 1G), the same observation was made in the presacrals II and III in the female.

Sacrum: The diapophyses of the sacrum are slightly longer than that of the presacral II, and moderately dilated and incline posterolaterally. Posteriorly, the sacrum bears a pair of condyles, which articulates with the urostyle.

Urostyle: The rod-shaped urostyle is approximately equal to the length of the whole trunk vertebrae. Dorsally, the urostyle bears a prominent longitudinal crest. The longitudinal crest is largest anteriorly and gradually decreases posteriorly.

3.1.3 Sternum The sternum at the midventral aspect of the chest is formed by the following parts (Figure 1H).

Episternum: The episternum presents as an anchor-shaped cartilage. Its anterior part is expanded and free, whereas its posterior part is thin and articulates with the omosternum.

Omosternum: The omosternum is bony, long, and wider posteriorly than it is anteriorly. The posterior end of the bone is fan-shaped and connects with the procoracoids.

Mesosternum: The length of the mesosternum is almost equal to that of the omosternum, but is much wider. Anteriorly, the mesosternum articulates with the coracoids and the epicoracoids. Posteriorly, it articulates with the xiphisternum.

Xiphisternum: The cartilaginous xiphisternum has a W-like shape. Its posterior end bears a narrow incision and the lateral border extends anterolaterally.

3.2 Appendicular Skeleton

3.2.1 Pectoral Girdle The pectoral girdle of *Q. robertingeri* has a firmisternal condition and consists of 7 paired elements as follows (Figure 1H).

Suprascapulae: The dolabriform suprascapula is the largest elements, and forms the dorsal part of the pectoral girdle. Its medial border articulates with the scapula,

while the lateral end is broadly expanded and free.

Cleithrums: The cleithrum is bony, bulb-shaped, and overlies most of the anterior and medial parts of the suprascapula. It covers nearly 30% of the suprascapula.

Scapulae: The scapula has an hour-shape and forms the anterolateral part of the pectoral girdle. The element articulates with the clavicle and the coracoid medially, which forms the anterior and the medial parts of the glenoid fossa. Laterally, it joins with the suprascapula and the cleithrum.

Clavicles: The slender clavicles is slightly bowed, points anteromedially, and is distinctly longer than the scapula. The clavicle constitutes the anterior part of the pectoral girdle. The bones are separated from one another medially and laterally articulate with the scapulae and the coracoids. In addition, there is a groove located at the dorsal and posterior part of the clavicle, which houses the procoracoid.

Coracoids: The coracoid has a trumpet-like shape. It is slightly longer than the clavicle and the scapula. Its medial side is striking expansive, and connects with the epicoracoid. The lateral end is narrow, and articulates with the clavicle and scapula, which creates the medial margin of the glenoid fossa.

Procoracoids: The procoracoids touch one another medially, extend along the dorsal posterior of the clavicles, and distally articulate with the scapulae.

Epicoracoids: The epicoracoid is fused to its counterpart on the midline, which forms a firmisternal arrangement. There is no distinct boundary between the procoracoids and the epicoracoids.

3.2.2 Pelvis Girdle The pelvis girdle is constituted by the paired ilia, the ischia and the pubes. Functionally, they provide a connection for the hind limbs and the vertebral column (Figure 1I, J, K).

Ilia: The ilia are characterized by elongated ilial shafts, which connect with the ventral surface of the sacral diapophyses anteriorly. Dorsally, each ilial shaft bears a longitudinal crest and a distal sesamoid. The posterior portion is expansive and forms the anterior half of the acetabulum.

Ischia: The fused ischia have an oval-like shape. They are synostotically united with the ilia and the pubes, which form the posterior half of the acetabulums.

Pubes: The fused pubes lie between the ilia and the ischia. They constitute the ventral parts of the acetabulums.

3.2.3 Forelimb **Humeri:** The humerus is the longest element of the forelimb. It embeds into the glenoid cavity proximally, and distally articulates with the radioulna

(Figure 1L, M). Compared with the female, the humerus of the male is much more robust, because the crista ventralis, the crista medialis, and the crista lateralis are more developed (Figure 1N, O).

Radioulnas: The preaxial radius and postaxial ulna are fused together and form the compound radioulna. The proximal end is modified by the capitulum and the olecranon, and articulates with the humerus, which forms the elbow joint. The distal end is relatively flat, and articulates with the radiale and the ulnare, which forms the wrist joint (Figure 1P).

Carpals: The carpal arrangement has Fabrezi's (1992) morphology "C", with a large element Y, radiale and ulnare in a medial to lateral sequence. The distal carpal 2 is synostotically united to the element Y proximally. Distally, it articulates with the metacarpal II. The fused distal carpal 3–5 is the largest, and lies between the radiale and ulnare and the base of the metacarpals II–V (Figure 1P).

Metacarpals: Metacarpals II–V are distinctly expansive at the proximal and distal ends, and medially slender. More importantly, the metacarpal II of the male is much more robust than the female. Additionally, the medial surface of the metacarpal II in the male bears a nuptial tuber that consists of 3 bony protuberances (Figure 1Q); this structure is absent in the female (Figure 1P).

Phalanges: The phalangeal formula is 2–2–3–3 for digits II–V, and the relative lengths of the digits are $IV > V > II > III$. Interestingly, the distal tips of the terminal phalanges end in an anchor-shape (Figure 1P).

Prepollex: The prepollex lies lateral to the element Y. It is formed by 2 elements, of which the distal element is much longer. The prepollex of the male is apparently larger and closer to the metacarpal II than that of the female (Figure 1P, Q).

3.2.4 Hind Limb **Femurs:** The femur is slightly sigmoid. Its proximal femoral head embeds into the acetabulum and distally articulates with the tibiotibula (Figure 1R).

Tibiofibulas: The tibiofibula is distinctly longer than the femur. A pair of nutrient foramina are located dorsally and ventrally in the central of the tibiofibula; however, their relative positions are different (Figure 1S).

Tarsals: The inner tibiale and outer fibulare are parallel and fused at the proximal and distal ends. The element Y is medially concave, laterally convex, and lies medial to the prehallux. The distal tarsal I is diminutive and adjacent to the base of the metatarsal I. The distal tarsals 2–3 are fused, large, and attached to the base of the metatarsals II–III (Figure 1T).

Metatarsals: The hind limb is characterized by 5

metatarsals. Their relative lengths are $IV > III > V > II > I$ (Figure 1T).

Phalanges: There are 5 toes on the foot, totally consisting of 14 phalangeal elements with the arrangement 2–2–3–4–3 for digits I–V. The relative lengths of the digits are $IV > III > V > II > I$ (Figure 1T). The distal tips of the terminal phalanges exhibit an anchor-like shape (Figure 1U).

Prehallux: The prehallux lies medial to the toe I, and is formed by 3 rectangular elements. The proximal element is large, whereas the other two elements decrease in size distally (Figure 1T).

4. Discussion

Based on the available literature, the osteology of *Q. robertingeri* was compared with other species in Dicroglossidae. According to Dubois (1975), *Q. spinosa* (Dicroglossidae: *Quasipaa*) is distinguished from *Q. robertingeri* by several osteological characteristics, and below are some examples of these characteristics: the maxillary process of the nasal of *Q. spinosa* is much longer and thinner, and forms almost the entire anterior margin of the orbit; the episternum has an expanded C-shape; the xiphisternum is larger and round; the omosternum, the mesosternum, the clavicles, and the coracoids are remarkably broader and more robust. Compared with *Q. robertingeri*, the diagnoses of *Paa liebigii* (Dicroglossidae: *Paa*) are as follows: the nasals are roughly L-shaped, separated from one another medially, posteriorly, they are not in contact with the frontoparietals; the sphenethmoid is partly exposed in the dorsal view; the maxillary process of the nasal is broad and laterally reaches two-thirds of the anterior margin of the orbit; the episternum is T-shaped, the xiphisternum is roughly triangular; the clavicle is straight, and perpendicular to the body axis (Dubois, 1975). Osteological features of *Yerana yei* (Dicroglossidae: *Yerana*) that are apparently different from *Q. robertingeri* are the following: the dentigerous processes of the vomers extend posteromedially, surpass the posterior terminus of the palatines, and posteriorly connect with the cultriform process of the parasphenoid; the episternum is sword-shaped; the length of the mesosternum is approximately 2 times that of the omosternum; the xiphisternum has a disc-like shape (Jiang *et al.*, 2006). Osteological characteristics of *Nanorana parkeri*, *N. pleskei*, and *N. ventripunctata* (Dicroglossidae: *Nanorana*) that distinctly differ from *Q. robertingeri* are the following: the nasals are separated from one other medially, and posteriorly not

connected with the frontoparietals; the sphenethmoid is partly exposed dorsally; the frontoparietals are formed by 2 detached elements, and the sagittal suture is relatively broad; the dentigerous processes of the vomers bear either a few vomerine teeth or none at all; the dentaries are tube-shaped anteriorly, and enclose the Meckel's cartilages; the mentomeckelians are cartilaginous (Wen, 2006). Based on similarities and distinctions of osteology, we conclude that *Q. robertingeri* has a closer relationship to *Q. spinosa* than it does to *Yerana yei*, we also conclude that *Paa liebigii*, *Nanorana parkeri*, *N. pleskei*, and *N. ventripunctata* have a closer relationship, which is consistent with available molecular data (Che *et al.*, 2009; Jiang *et al.*, 2006)

Among amplexant anurans, the forelimbs of males frequently present a series of unique traits. For instance, the preaxial 2 or 3 fingers of male *Q. robertingeri* bear prominently black nuptial spines (Chen *et al.*, 2010a, 2010b; Epstein and Blackburn, 1997; Fei *et al.*, 2009; Wells, 2007). Furthermore, the humerus of the male *Q. robertingeri* exhibits strikingly larger crista ventralis, crista medialis and crista lateralis- similar to the humeri of *Q. spinosa* and *Paa liebigii* (Dubois, 1975). The sexual dimorphism in the forelimb bones is most likely correlated to amplexus. For instance, the deltoid muscle, flexes the shoulder joint by pulling the humerus forward, and distally inserts the crista ventralis. Moreover, the flexor carpi radialis muscle, the main flexor of the hand, originates from the crista medialis. The flexor antibrachii lateralis superficialis muscle, arises from the crista lateralis and lateral epicondyle of the humerus, and plays a significant role in flexing the elbow, and extending and supinating the hand (Duellman and Trueb, 1986; Feng, 1988; Zhou, 1956). Additionally, larger crests could potentially increase the surface of the humerus and accordingly allow for the attachment of more musculature (Trueb, 1973). Similarly, the nuptial tuber of the male *Q. robertingeri*, coupled with the larger prepollex, presumably increases the clasping area, enhances the amplexant strength, and thus improves the ability of males to mate successfully.

Anurans contact the ground or substrate with manus and pes. As such, the distal ends of their ultimate phalanges have been modified into various shapes (Duellman and Trueb, 1986; Kent and Miller, 1997; Lynch, 1969; Tihen, 1965; Trueb, 1973). For the terrestrial species of *Bofu gargarizans* and *B. stejnegeri* (Anura: Bufonidae), the distal tips of terminal phalanges are blunt and well suited to the flat land (Feng, 1988; Liu *et al.*, 2010). *Rugosa emeljanovi* (Anura: Ranidae) lives in still

water, and its terminal phalanges distally expand into knot-like shape that provides them with more stability (Wu and Zhao, 2006). *Q. robertingeri* inhabits streams, and the distal ends of its terminal phalanges are anchor-shaped, which helps them keep balance when they jump in streams or surrounding riparian areas. The distal phalanges of arboreal species have a Y-shaped bifurcation. Combined with the distal intercalary elements, the fingers and toes are better able to grasp the substrate more firmly and flexibly (Fei *et al.*, 2009). We believe that different environments that cause terminal phalanges to evolve into diverse shapes.

Acknowledgements Financial support was provided by the National Natural Science Foundation of China (NSFC) to Xiaohong CHEN (Grant Nos. 30870277, 31372164, 31572245), the key discipline of ecology of Henan Province, and the innovation team of science and technology of Henan Province (C20140032).

References

- Che J., Hu J. S., Zhou W. W., Murphy R. W., Papenfuss T. J., Chen M. Y., Rao D. Q., Li P. P., Zhang Y. P. 2009. Phylogeny of the Asian spiny frog tribe Paini (Family Dicroglossidae) sensu Dubois. *Mol Phylogenet Evol*, 50: 59–73
- Chen X. H., Zhou K. Y., Zheng G. M. 2010a. A new species of the genus *Odorrana* from China (Anura, Ranidae). *Acta Zootaxon Sin*, 35: 206–211 (In Chinese)
- Chen X. H., Zhou K. Y., Zheng G. M. 2010b. A new species of Odor frog from China (Anura: Ranidae). *J Beijing Normal Univ (Nat Sci)*, 46: 606–609 (In Chinese)
- Dubois A. 1975. Un nouveau sous-genre (*Paa*) et trois nouvelles espèces du genre *Rana*. Remarques sur la phylogénie des Ranidés (Amphibiens, Anoures). *Bull Mus Natn Hist Natl, Paris* (3) 324: 1093–1115
- Dubois A. 1992. Notes sur la classification des Ranidae (Amphibiens Anoures). *Bull Mens Soc Linn Lyon*, 61: 305–352
- Dubois A. 2005. *Amphibia Mundi 1.1: An ergotaxonomy of recent amphibians*. *Alytes*, 23(1–2): 1–24
- Duellman W. E., Trueb L. 1986. *Biology of amphibians*. New York: McGraw-Hill Book Company, 289–365
- Epstein M. S., Blackburn D. G. 1997. Histology and histochemistry of androgen-stimulated nuptial pads in the leopard frog, *Rana pipiens*, with notes on nuptial pad evolution. *Can J Zool*, 75: 472–477
- Fabrezi M. 1992. El carpo de los anuros. *Alytes*, 10: 1–29
- Fei L., Hu S. Q., Ye C. Y., Huang Y. Z. 2009. *Fauna Sinica, Amphibia, Vol. 3. Anura Ranidae*. Beijing, China: Science Press (In Chinese)
- Fei L., Ye C. Y., Jiang J. P. 2012. *Colored Atlas of Chinese Amphibians and Their Distributions*. Chengdu, China: Sichuan Publishing House of Science and Technology (In Chinese)
- Feng X. Y. 1988. *The systematic dissection of Bofu gargarizans*. Beijing, China: Higher Education Press, 5–22pp (In Chinese)

- Huang J., Luo J., Song J. Q., Wang Z. J.** 2010. New records of two amphibian species *Quasipaa robertingeri* and *Odorrana hejiangensis* in Chongqing. *Chin J Zool*, 45(2): 158–161
- Hoyos J. M., Medina P., Schoch P.** 2015. Osteology of *Atelopus muisca* (Anura, Bufonidae) from Colombia. *Zootaxa*, 3905: 119–130
- Inger R. F.** 1967. The development of a phylogeny of frogs. *Evolution*, 21: 369–384
- Jorgensen M. E., Reilly S. M.** 2013. Phylogenetic patterns of skeletal morphometrics and pelvic traits in relation to locomotor mode in frogs. *J Evol Biol*, 26: 929–943
- Jiang J. P., Chen X. H., Wang B.** 2006. A new genus of family Ranidae from China-*Yerana* (Ranidae: Dicroglossinae). *J Anhui Normal Univ (Nat Sci)*, 5: 467–469 (In Chinese)
- Kent G. C., Miller L.** 1997. Comparative anatomy of the vertebrates. New York: McGraw-Hill Book Company, 136–259pp
- Lehr E., Trueb L.** 2007. Diversity among New World microhylid frogs (Anura: Microhylidae): morphological and osteological comparisons between *Nelsonophryne* (Günther 1901) and a new genus from Peru. *Zool J Linn Soc*, 149: 583–609
- Liu Y., Lu Y. Y., Li P. P., Xu Q. Y.** 2010. Study on osteology of *Bufo stejnegeri*. *J Life Sci*, 4: 27–34 (In Chinese)
- Li C., Zhang Z. D., Wen T., Peng H., Guo P.** 2009. A new record of amphibian in Yunnan province: *Quasipaa robertingeri*. *Sichuan J Zool*, 28(6): 923–924 (In Chinese)
- Lynch J. D.** 1969. Evolutionary relationship and osteology of the frog family Leptodactylidae. Ph.D. Thesis, University of Kansas
- Scott E.** 2005. A phylogeny of ranid frogs (Anura: Ranoidea: Ranidae), based on a simultaneous analysis of morphological and molecular data. *Cladistics*, 21(6): 507–574
- Simons V. F. H.** 2008. Morphological correlates of locomotion in Anurans: limb length, pelvic anatomy and contact structures. MSc Thesis. Ohio University. 87pp
- Tihen J. A.** 1965. Evolutionary trends in frogs. *Am Zool*, 5: 309–318
- Trewavas E.** 1933. The hyoid and larynx of the Anura. *Phil Trans R Soc London*, 222: 401–527
- Trueb L.** 1973. Bones, frogs and evolution. In: Vial, J.L. (Eds.), *Evolutionary Biology of the Anurans: Contemporary research on major problems*, Columbia: University of Missouri Press, 65–132pp
- Wang S., Xie Y.** 2009. China species red list, Vertebrates Part1. Beijing, China: Higher Education Press, 704pp (In Chinese)
- Wei G., Wang B., Xu N., Li Z. Z., Jiang J. P.** 2009. Morphological evolution from aquatic to terrestrial in the genus *Oreolalax* (Amphibia, Anura, Megophryidae). *Prog Nat Sci*, 19: 1403–1408
- Wells K. D.** 2007. The ecology and behavior of amphibians. Chicago: University of Chicago Press
- Wen X. M.** 2006. Studies on the osteology of genus *Nanorana* (Anura: Dicroglossinae). M.S. Thesis. Sichuan University. 47pp (In Chinese)
- Wu G. F., Zhao H.** 2006. Study on skeletal system of *Rana rugosa* Temmick et Schegel. *Sichuan J Zool*, 25: 218–222 (In Chinese)
- Xiong J. L.** 2008. The comparative anatomy of skeleton of the Chinese Hynobiidae salamanders and description of a new genus. Ph.D. Thesis. Sichuan University. 184pp
- Zhou B. X.** 1956. The anatomy of the frog. Beijing, China: Science Press, 55–72pp (In Chinese)